Characterization of Kinetic and Thermodynamic Parameters of Cyanidin-3-glucoside Methyl and Glucuronyl Metabolite Conjugates

ARTICLE *in* THE JOURNAL OF PHYSICAL CHEMISTRY B · JANUARY 2015

Impact Factor: 3.3 · DOI: 10.1021/jp511537e · Source: PubMed

THE JOURNAL OF PHYSICAL CHEMISTRY B

Article

pubs.acs.org/JPCB

Characterization of Kinetic and Thermodynamic Parameters of Cyanidin-3-glucoside Methyl and Glucuronyl Metabolite Conjugates.

Luís Cruz,[†] Nuno Basílio,[‡] Nuno Mateus,[†] Fernando Pina,*[,‡] and Victor de Freitas*[,†]

[†]Centro de Investigação em Química e Bioquímica, Departamento de Química, Faculdade de Ciências, Universidade do Porto, Rua do Campo Alegre, 687, 4169-007 Porto, Portugal

[‡]REQUIMTE, Departamento de Química, Faculdade de Ciências e Tecnologia, Universidade Nova de Lisboa, 2829-516 Monte de Caparica, Portugal

ABSTRACT: The determination of rate and equilibrium constants of anthocyanin metabolites with *in vivo* occurrence, cyanidin-4′-*O*-methyl-3-glucoside (Cy4′Me3glc) and cyanidin-7-*O*-glucuronyl-3-glucoside (Cy7Gluc3glc), was carried out for the first time by means of direct and reverse pH jumps. The thermodynamics and kinetics of these compounds are similar to the anthocyanin monoglucosides in particular for the analogous cyanidin-3-glucoside (Cy3glc) and peonidin-3-glucoside (Peo3glc). The rate and equilibrium constants of metabolites were also compared with malvin (malvidin 3,5-diglucoside) and with a bioinspired compound 3′,4′-dihydroxy-7-*O*-glucopyranosyloxyflavylium (DGF). In Cy4′Me3glc and Cy7Gluc3glc the rate of hydration for a fixed pH value is slower than in DGF and the dominant species at moderately acidic solutions is the hemiketal. Oppositely, in DGF *trans*-chalcone is the dominant species at moderately acidic solutions.

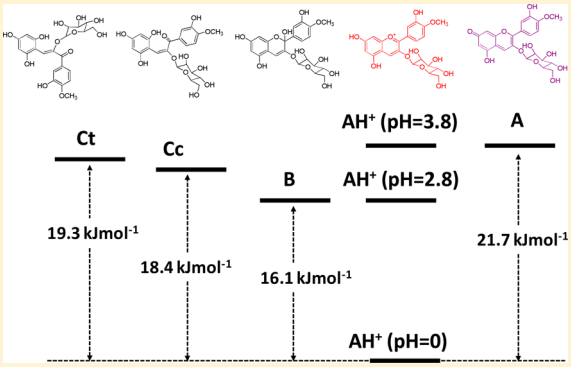

1. INTRODUCTION

Anthocyanins are a family of polyphenolic compounds widespread in many plant foods and processed beverages such as red wine and red fruit juices.[1] *In vitro* studies on their biological activities have demonstrated that anthocyanins may offer potential beneficial effects to human health due to their antioxidant potential and reported antitumor, antimicrobial, and anti-inflammatory actions.[2−6] Nowadays, it is recognized that the *in vivo* anthocyanin bioactive forms do not always correspond to the native forms but conjugates or metabolites arising from them after absorption.[7] In fact, anthocyanins are rapidly absorbed in the stomach[8] and small intestine,[9] and then they appear in blood circulation and urine as intact, methylated, glucurono- and/or sulfoconjugated forms.[10−12] For those reasons, the study of the biological properties of anthocyanin metabolites has attracted great interest from the scientific community. Like anthocyanins, their metabolites are also present in aqueous solution under different equilibrium forms depending on the pH of the medium.[13,14] Metabolites in the human organism find different environments which will affect the species present in equilibrium such as the stomach (pH < 4) and the intestine, plasma, tissues, and organs (pH ≈ 7). Thus, it is important to know their kinetic−thermodynamic parameters in order to identify which species are present in equilibrium and to make a correct quantification of these compounds in different biological matrices.

Anthocyanins and related flavylium compounds follow the same network of chemical reactions regardless of their natural or synthetic origin. According to the nature and position of the flavylium substituents, the thermodynamics and kinetics of the flavylium network of chemical reactions changes dramatically.

When anthocyanins are compared with some synthetic flavylium compounds or even with those of natural provenience, such as 4′,7-dihydroxyflavylium,[15] it is observed that the mole fraction distribution of the network species is very dependent on the substitution pattern. While the thermodynamic and kinetic information regarding synthetic flavylium derivatives with hydroxyl and methoxy groups in several positions of the flavylium core are available, there is a lack of studies on synthetic derivatives bearing sugar substituents. The presence of sugars in the flavylium core confers more solubility of the compounds in water and defines a bioinspired strategy of synthesis. This is precisely the case for the anthocyanin metabolites.

In this work, the kinetic and thermodynamic parameters of two synthesized anthocyanin metabolites with *in vivo* occurrence, Cy4′Me3glc and Cy7Gluc3glc, were studied and the results compared with natural anthocyanins and synthetic bioinspired compounds such as 3′,4′-dihydroxy-7-*O*-glucopyranosyloxyflavylium (DGF).

2. EXPERIMENTAL SECTION

2.1. Synthesis. *2.1.1. Cyanidin-4′-O-methyl-3-glucoside (Cy4′Me3glc).* This metabolite was synthesized through an acidic

Received: November 18, 2014
Revised: January 8, 2015
Published: January 9, 2015

DOI: 10.1021/jp511537e
J. Phys. Chem. B 2015, 119, 2010−2018

aldol condensation between compounds **1** and **2** according to the procedures reported in the literature.[16]

*2.1.2. 2,6-Dihydroxy-4-(2,3,4-tri-O-acetyl-α-D-glucopyranuronic acid methyl ester)benzaldehyde (**3**).* 2,4,6-Trihydroxybenzaldehyde (0.52 mmol, 80 mg) and bromo-2,3,4-tri-*O*-acetyl-α-D-glucopyranuronic acid methyl ester (1.5 equiv) were mixed with an excess of silver carbonate (3 equiv) in anhydrous toluene. The reaction was stirred at 100 °C for 5 h. The reaction was then filtered, the solvent removed under vacuum, and the product extracted with ethyl acetate and water. Flash column chromatography (DCM:MeOH 10:1) gave the final compound as pale yellow oil (40% of yield).

^{1}H NMR (400.14 MHz, $CDCl_3$), δ (ppm): 9.95 (s, 1H, CHO), 6.07 (s, 2H), *glucuronic acid*, 5.60 (d, *J* = 9.7 Hz, 1H, H-1′), 5.18 (d, *J* = 9.4 Hz, 1H, H-5′), 4.92−4.24 (*, 3H, H-2′, H-3′, H-4′), 3.76 (s, 3H, COOMe), 2.04 (s, 9H, OCOMe). ESI−MS *m*/*z*: 469 $[M\text{-}H]^-$.

*2.1.3. 2-(2,3,4,6-Tetra-O-acetyl-β-D-glucopyranosyloxy)-3′,4′-diphenylmethylenedioxyacetophenone (**4**).* Compound **4** was synthesized through three steps from the starting material 2-chloro-3′,4′-dihydroxyacetophenone following the procedures reported elsewhere.[17]

2.1.4. Cyanidin-7-O-glucuronyl-3-glucoside (Cy7Gluc3glc). 2,6-Dihydroxy-4-(2,3,4-tri-*O*-acetyl-α-D-glucopyranuronic acid methyl ester)benzaldehyde **3** (0.1 mmol, 47 mg) and 2-(2,3,4,6-tetra-*O*-acetyl-β-D-glucopyranosyloxy)-3′,4′-diphenylmethaneacetophenone **4** (0.1 mmol, 66.4 mg) were dissolved in dry EtOAc (5 mL), and anhydrous HCl (g) was bubbled through the solution. The reaction was stirred from 0 °C to room temperature, and a red color gradually developed. The mixture was then stirred until all of the starting materials were consumed as monitored by TLC. No purification was undertaken at this stage. The solvent was evaporated and the residue dissolved in MeOH. Complete deacetylation was performed with KOH (3 equiv) in MeOH/H_2O 1:1. The mixture was stirred at room temperature for 15 min and then carefully acidified to pH 1 with HCl 1M. After MeOH evaporation, the aqueous solution was filtered to remove the majority of KCl precipitate and further extracted with ethyl acetate to remove benzophenone molecule and other impurities that have maximum absorbance wavelenghts in the UV region. The metabolite was further eluted on silica gel C18-reversed phase to remove the acetic acid, and the desired compound was recovered in acidic MeOH. The MeOH was removed and the residue was purified by column chromatography using TSK Toyopearl HW-40 (S) gel (150 mm × 16 mm i.d.). The metabolite was eluted with water acidified with 2% HCl at flow rate at 0.8 mL/min. After concentration, the purity of metabolite was checked by HPLC-DAD. The full structural characterization was achieved by LC-DAD/ESI−MS and NMR.

^{1}H NMR (600.13 MHz, CD_3OD/TFA 98:4), δ (ppm): 9.14 (s, 1H, H-4C), 8.37 (dd, 2.2/8.7 Hz, 1H, H-6′B), 8.10 (d, 2.2 Hz, 1H, H-2′B), 7.12 (d, *J* = 1.5 Hz, 1H, H-8A), 7.05 (d, 8.7 Hz, 1H, H-5′B), 7.00 (d, *J* = 1.5 Hz, 1H, H-6A); *Glucose*, 5.32 (d, *J* = 7.7 Hz, 1H, H-1″), 3.96 (*, 1H, H-6a″), 3.72 (*, 1H, H-6b″), 3.69 (*, 1H, H-2″), 3.64 (*, 1H, H-5″), 3.57 (*, 1H, H-3″), 3.42 (*, 1H, H-4″); *glucuronic acid*, 5.29 (d, *J* = 7.6 Hz, 1H, H-1‴), 4.18 (d, *J* = 9.7 Hz, 1H, H-5‴), 3.73 (*, 1H, H-2‴), 3.68 (*, 1H, H-4‴), 3.58 (*, 1H, H-3‴). ^{13}C NMR (125.77 MHz, CD_3OD/TFA 98:4), δ (ppm): 167.7 (C-7A), 163.8 (C-2C), 155.8 (C-4′B, C-8aA), 154.9 (C-5A), 146.2 (C-3′B), 145.3 (C-3C), 134.4 (C-4C), 127.6 (C-6′B), 119.8 (C-1′B), 117.0 (C-2′B), 116.0 (C-5′B), 112.0 (C-4aA), 104.1 (C-6A), 96.0 (C-8A); *glucose*, 102.3 (C-1″), 75.4 (C-3″), 73.1 (C-2″), 71.3 (C-5″), 69.8 (C-4″), 60.9 (C-6″); *glucuronic acid*, 169.5 (COOH), 100.8 (C-1‴), 75.5 (C-5‴), 75.3 (C-3‴), 73.6 (C-2‴), 73.0 (C-4″). LC-DAD/ESI−MS *m*/*z*: 625 $[M]^+$.

2.2. HPLC-DAD. HPLC analyses were performed on a Merck-Hitachi L-7100 (Merck, Darmstadt, Germany) apparatus with a 150 × 4.6 mm i.d. reversed-phase ODS C18 column (Merck, Darmstadt) at 25 °C; detection was carried out using a L-7450A diode array detector (DAD). The eluents were (A) H_2O/HCOOH (9:1) and (B) CH_3CN. The gradient consisted of 0−35% B for 50 min at a flow rate of 0.5 mL/min. The column was washed with 100% B during 10 min and then stabilized with the initial conditions during another 10 min.

2.3. LC-DAD/ESI−MS. LC-DAD/ESI/MS analyses were performed on a Finnigan Surveyor series liquid chromatograph equipped with Finnigan LCQ (Finnigan Corp., San Jose, CA) mass detector and an API source using an ESI interface. The samples were analyzed on a reversed-phase column (150 × 4.6 mm, 5 μm, C18) at 25 °C using the same eluents, gradients and flow rates referred for HPLC analysis. The capillary voltage was 4 V and the capillary temperature 275 °C. Spectra were recorded in positive and negative ion modes between *m*/*z* 120 and 1500. The mass spectrometer was programmed to do a series of three scans: a full mass (MS), a zoom scan of the most intense ion in the first scan (MS^2), and a MS−MS of the most intense ion using relative collision energy of 30 and 60 (MS^3).

2.4. NMR. ^{1}H NMR (600.13 MHz) and ^{13}C NMR (125.77 MHz) spectra were recorded in CD_3OD/TFA (98:4) on a Bruker-Avance 600 spectrometer at 303 K and with TMS as an internal standard (chemical shifts (d) in parts per million, coupling constants (J) in hertz). Multiplicities are recorded as singlets (s), doublets (d), triplets (t), doublets of doublets (dd), multiplets (m) and unresolved (*). ^{1}H chemical shifts were assigned using 2D NMR (COSY) experiment while ^{13}C resonances were assigned using 2D NMR techniques (gHMBC and gHSQC). The delay for the long-range C/H coupling constant was optimized to 7 Hz.

2.5. UV−vis Spectroscopy. The pH of the solutions was adjusted by addition of HCl, NaOH or universal buffer of Theorell and Stenhagen[18] and pH was measured in a Radiometer Copenhagen PHM240 pH/ion meter. UV−vis absorption spectra were recorded in a Varian-Cary 100 Bio or 5000 spectrophotometer. Direct pH jumps were carried out by addition of the necessary amount of base and buffer (tipically 2 mL) to get the desired final pH, from a previous equilibrated solution of flavylium cation at pH = 1.0 (1 mL). This way the stock solution of compound is diluted by a factor of 3 upon a direct pH jump. The final concentration of Cy4′Me3glc was 3.3×10^{-5} M and of Cy7Gluc3glc was 9×10^{-6} M. Anthocyanins and their derivatives are known to aggregate but under these conditions the fraction of aggregated molecules is not relevant.[19] The reverse pH values were performed from equilibrated solutions at moderately acidic pH values back to very acidic pHs. All the fitting procedures were carried out using the program solver from excel.

2.6. Stopped Flow. Stopped-flow experiments were conducted in an Applied Photophysics SX20 stopped-flow spectrometer provided with a PDA.1/UV photodiode array detector with a minimum scan time of 0.65 ms and a wavelength range of 200 to 735 nm. For direct pH jumps, stock solutions of the compound at pH 1 are placed in one syringe and the necessary amount of base and buffer to obtain the desired final pH in another syringe. Upon mixing the concentration of the compound is diluted by a factor of 2. Similarly, reverse pH jump are carried out by placing an equilibrated solution of the compound

DOI: 10.1021/jp511537e
J. Phys. Chem. B 2015, 119, 2010−2018

Scheme 1. Chemical Synthesis Strategies to Obtain the Two Cyanidin-3-glucoside Metabolite Derivatives

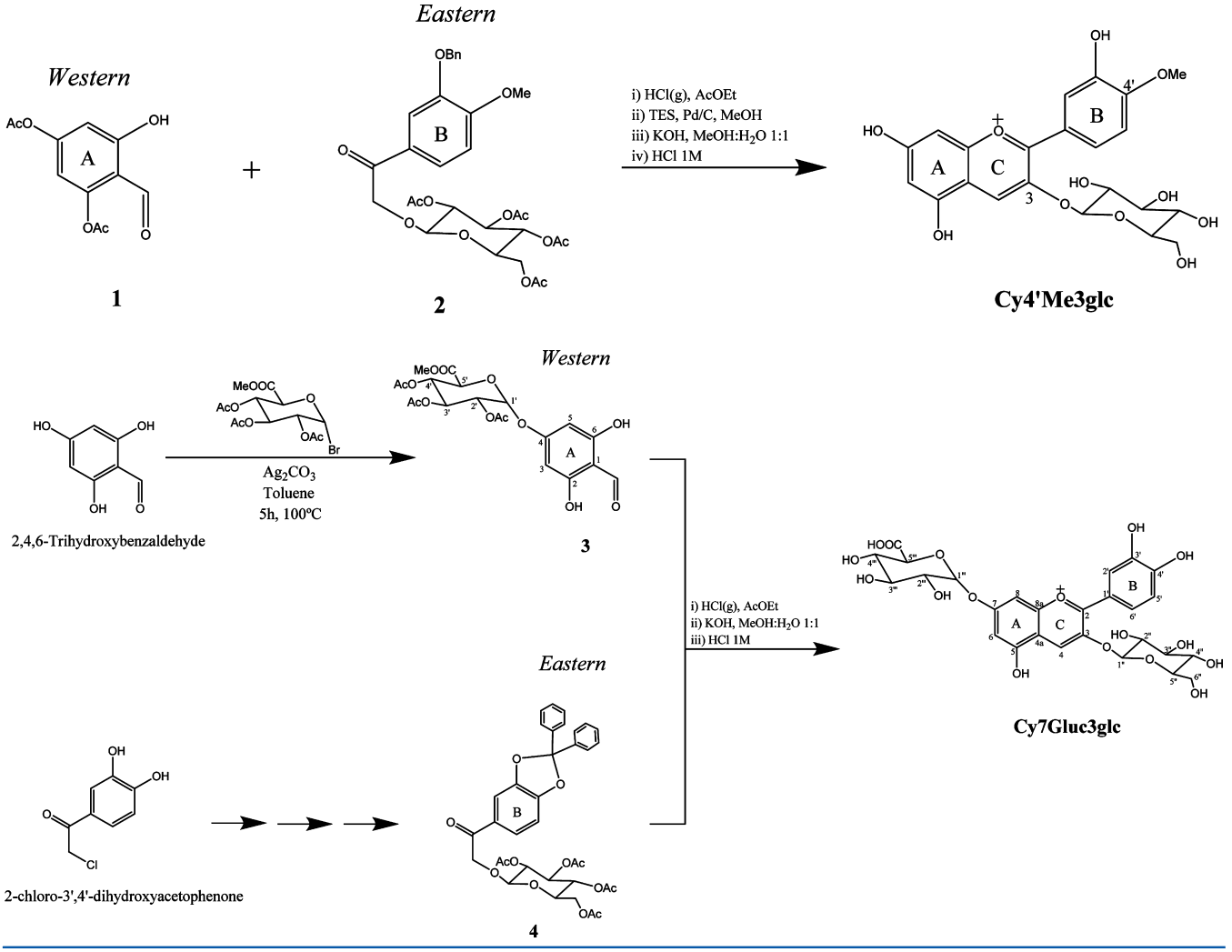

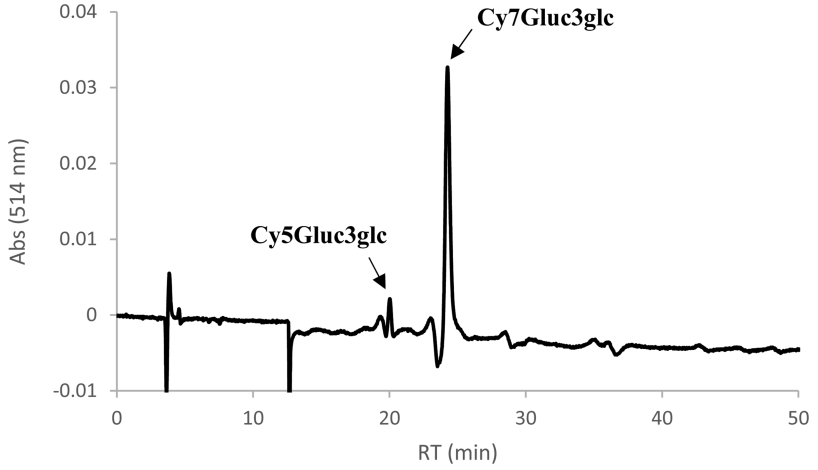

Figure 1. HPLC chromatogram recorded at 514 nm of cyanidin-3-glucoside glucuronic conjugates after Toyopearl gel purification.

at a given pH in one syringe and the respective amount of HCl in the second syringe to obtain the desired final pH values. A small volume of sample is recovered after mixing to confirm the pH.

3. RESULTS AND DISCUSSION

3.1. Metabolites Synthesis. Overall, the strategy adopted for the synthesis of cyanidin-3-glucoside metabolite derivatives involved first the preparation of the A and B rings, denominated the "*western*" and "*eastern*" parts of the molecule, respectively, and then the construction of the C-ring by cyclization (Robinson's acidic aldol condensation) (Scheme 1).

To obtain compound **3**, a glucuronylation reaction of 2,4,6-trihydroxybenzaldehyde was performed directly without protection of hydroxyl groups. Because of the strong hydrogen bonds

DOI: 10.1021/jp511537e
J. Phys. Chem. B 2015, 119, 2010−2018

Scheme 2. Network of Chemical Reactions of Cyanidin-3-glucoside

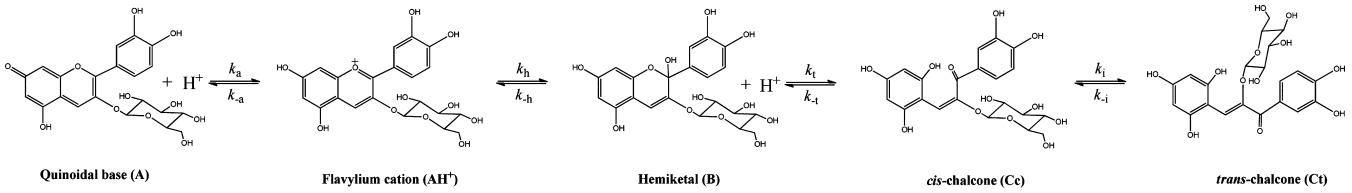

between the carbonyl group and C2−OH and C6−OH of 2,4,6-trihydroxybenzaldehyde, the latter groups are much less acidic than C4−OH. Therefore, the glucuronylation reaction to obtain took place more selectively to the C4−OH.[20] Direct injection in mass spectrometry (ESI−MS) in negative ion mode gave the pseudomolecular ion $[M\text{-}H]^-$ at m/z 469 which is compatible with the molar mass of the desired compound. Furthermore, this pseudomolecular ion produces the MS^2 ions at m/z 427, 409, 367, 349, and 153, which are in concordance with the fragmentation pattern for this structure. Proton NMR of this molecule was then performed and indicated the presence of two singlets that were assigned to the proton of the aldehyde group. This confirmed that the glucuronylation reaction occurred in the C2-OH position although in very small extension.

After the acidic condensation reaction between **3** and **4** the mixture was analyzed directly in mass spectrometry in positive ion mode. The results gave molecular ions $[M]^+$ at m/z 891, 849, 807, 765 which indicated that the coupling had occurred as well as the partial deacetylation of the flavylium ions. MS^2 of all these molecular ions gave rise to the common ion $[M]^+$ at m/z 287, which corresponds to the cyanidin aglycone molecule (losses of glucoside and glucuronyl residues with different number of acetyl groups).

After complete protecting groups removal, acidification and purification procedures, the purity of metabolite was checked by HPLC-DAD (Figure 1).

LC-DAD/ESI−MS analysis of the mixture in positive ion mode confirmed the presence of two chromatographic peaks with the same molecular ion $[M]^+$ at m/z 625, which agrees with the flavylium cation of cyanidin-3-glucoside attached to a glucuronic acid. MS^2 fragments of this ion yielded $[M - 162]^+$ at m/z 463, corresponding to the glucuronyl aglycone (loss of glucose molecule), $[M - 176]^+$ at m/z 449, which corresponds to the loss of glucuronic acid and $[M - 338]^+$ at m/z 287, which represents the loss of both glucose and glucuronyl residues. The UV−vis spectrum of Cy7Gluc3glc agrees with the ones already reported.[21] The metabolite was freeze-dried and obtained as a red solid which was further fully characterized by ^1H and ^{13}C NMR.

3.2. Network of Equilibria Reactions of Anthocyanin-Related Compounds. Cyanidin-3-glucoside is used to illustrate the kinetic and thermodynamic of the network of chemical reactions taking place in anthocyanins (Scheme 2).

The global equilibrium is defined according to eqs 1−4:

$$\mathbf{AH}^+ + H_2O \rightleftharpoons \mathbf{A} + H_3O^+,\ K_a \text{ proton transfer} \quad (1)$$

$$\mathbf{AH}^+ + 2H_2O \rightleftharpoons \mathbf{B} + H_3O^+,\ K_h \text{ hydration} \quad (2)$$

$$\mathbf{B} \rightleftharpoons \mathbf{Cc},\ K_t \text{ tautomerization} \quad (3)$$

$$\mathbf{Cc} \rightleftharpoons \mathbf{Ct},\ K_i \text{ isomerization} \quad (4)$$

When the pH increases, from very acidic solutions containing the flavylium cation $\mathbf{AH}^+$, here on defined as direct pH jumps, two competitive reactions occur: (i) proton transfer of the hydroxyl in position 7 to give the quinoidal base **A**, (eq 1), (ii) hydration of the flavylium cation in position 2, leading to the hemiketal **B**, (eq 2). The hemiketal further undergoes a ring-opening/closure to give *cis*-chalcone **Cc** (tautomerization reaction, eq 3) which then isomerizes to *trans*-chalcone **Ct** (eq 4). The system is pH reversible and the flavylium cation is recovered by reacidification of the solutions previously equilibrated (or pseudoequilibrated) at moderately acid (or basic), here on defined as reverse pH jumps.

Proton transfer is by far the fastest reaction of the network but **A** it is not necessarily more stable than **B**. The relative energies of the three species $\mathbf{AH}^+$, **A**, and **B** are represented in Scheme 3,

Scheme 3. Thermodynamic Scheme of the Flavylium-Derived Compounds[a]

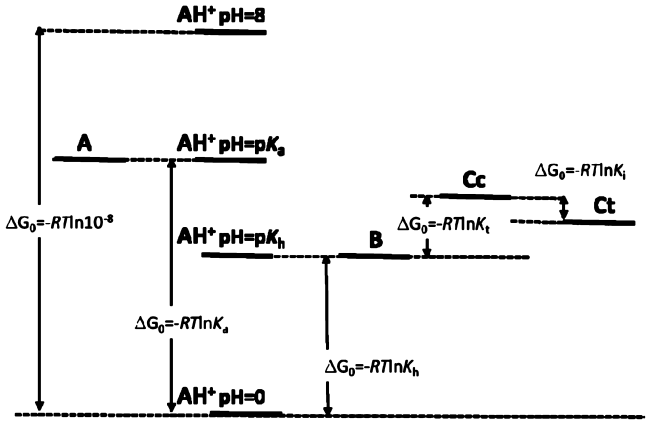

[a]The equilibrium constants are defined by $K_n = (k_n/k_{-n})$ (n = a, h, t, i), see eqs 1, 2, 3, and 4.

illustrating the case of the anthocyanins where **B** is thermodynamically more stable than **A, Cc**, and **Ct**.

In order to show the usefulness of Scheme 3, let consider a direct pH jump from a pH where the flavylium cation is the dominant species (for example pH = 1) to pH = pK_h. The main reaction will be the hydration because there is no thermodynamic access to **A**. This process is pH dependent and takes place from subseconds (very acidic pH) to several minutes; if the pH jump occurs at pH = pK_a, equal amounts of $\mathbf{AH}^+$ and **A** reach the equilibrium during the mixing time of the base. However, **A** is not more stable than **B** and by consequence it is a kinetic product that evolves to **B** (and this one subsequently to **Cc** and **Ct**). An important breakthrough of the system was reported by Brouillard and Dubois, who discovered that in acidic to neutral medium **A** is stable to the hydration.[22,23] In other words, only the fraction of $\mathbf{AH}^+$ that remains in equilibrium with **A** is responsible for the formation of **B**. In kinetic terms, while the rate of the proton transfer is given by eq 5 representing the forward and backward kinetic process observed for a reaction approaching the

DOI: 10.1021/jp511537e
J. Phys. Chem. B 2015, 119, 2010−2018

equilibrium, in the case of the hydration, eq 6, the subsequent reaction should be multiplied by the mole fraction of $\mathbf{AH}^+$ available to react.

$$k_{obs1} = k_a + k_{-a}[H^+] \tag{5}$$

$$k_{obs2} = \frac{[H^+]}{K_a + [H^+]} k_h + \frac{1}{1 + K_t} k_{-h}[H^+] \tag{6}$$

In eq 6, the backward constant is also multiplied by another mole fraction, representing the fraction of **B** available to react back to $\mathbf{AH}^+$. This is due to the fact that one faster reaction occurs due to the opening of the central ring in **B** to form a *cis*-chalcone, **Cc**.

The ring-opening/closure occurs in a time scale of subseconds and, except for very acidic pH values, it is much faster than hydration.

The last kinetic process in anthocyanins corresponds to the formation of *trans*-chalcone upon isomerization of the double bond. In anthocyanins the *cis*−*trans* isomerization is the slowest step of the network and by consequence all the species except **Ct** equilibrate before its significant formation, and the respective rate constant is given by eq 7 (for further details see reference Pina F., 2014).[24]

$$k_{obs3} = \frac{K_h K_t}{K_a + K_h K_t + [H^+]} k_i + k_{-i} \tag{7}$$

3.2.1. Cy4′Me3glc. The spectral variations of equilibrated solutions of the metabolite Cy4′Me3glc are shown in Figure 2.

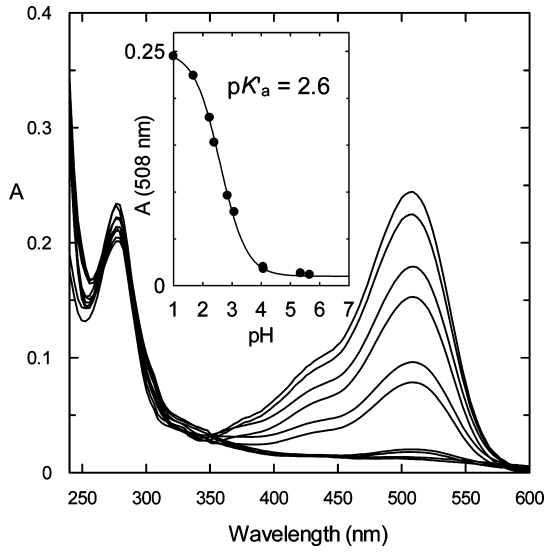

Figure 2. Spectral variations of the compound Cy4′Me3glc, 3.3×10^{-5} M, as a function of pH.

At low pH values, the absorption spectrum of $\mathbf{AH}^+$ is observed. As the pH increases the flavylium cation disappears giving place to other species absorbing in the UV region of the spectra. On the basis of the experimental data of hundreds of flavylium derivatives (natural and synthetic) the shape and position of these bands at higher pH values exclude the existence of significant amounts of **Ct**.[14] In particular the small absorption in the visible at higher pH values, red-shifted in comparison with the one of $\mathbf{AH}^+$, indicates the presence of a small fraction of **A**.

As shown previously, the network of chemical reactions can be simplified considering the equilibrium in eq 8, which results from the conjugation of eqs 1−4.

$$\mathbf{AH}^+ + H_2O \rightleftharpoons \mathbf{CB} + H_3O^+,$$
$$K'_a = K_a + K_h + K_h K_t + K_h K_t K_i \tag{8}$$

Equation 8 is equivalent to a single acid−base equilibrium between flavylium cation and a conjugate base, **CB**, defined as the sum of the concentrations of the other species of the network, $[\mathbf{CB}] = [\mathbf{A}] + [\mathbf{B}] + [\mathbf{Cc}] + [\mathbf{Ct}]$

The spectral variations shown in Figure 2 are compatible with eq 8 leading to a value of $pK'_a = 2.6$.

From the set of eqs 1, 2, 3, 4 and 8, it is easy to obtain the pH-dependent mole fraction distribution of the network species, eqs 9.

$$\chi_{\mathbf{AH}^+} = \frac{[H^+]}{[H^+] + K'_a}; \quad \chi_{\mathbf{A}} = \frac{K_a}{[H^+] + K'_a};$$
$$\chi_{\mathbf{B}} = \frac{K_h}{[H^+] + K'_a}; \quad \chi_{\mathbf{Cc}} = \frac{K_h K_t}{[H^+] + K'_a};$$
$$\chi_{\mathbf{Ct}} = \frac{K_h K_t K_i}{[H^+] + K'_a} \tag{9}$$

In Figure 3A, a direct pH jump from pH = 1.0 to 5.7 is shown. As expected, the initial absorbance is compatible with formation of the species **A**. Taking into account that the proton transfer is faster than the mixing time of the pH jump, the initial absorbance A_i corresponds to the total concentration of the anthocyanin in the form of **A**. The absorbance of the species **A** decreases with time to give the other "basic" forms of the network. On the other hand, the final absorbance in the visible, A_f, is due to the remaining **A** at the equilibrium. The ratio A_f/A_i is thus the mole fraction of the species **A** at the equilibrium at that pH value, eq 9, leading to $pK_a = 3.8$ from $pK'_a = 2.6$. Moreover it predicts the existence of *circa* 6% of base at the equilibrium, which is compatible with the data of Figure 2.

The decreasing of the absorbance with time occurs according to a first order kinetic process. As described above, this process corresponds to the transformation of $\mathbf{AH}^+/\mathbf{A}$ into **B** and **Cc**. Fitting of the absorption data to a single exponential equation allows the determination of the observed rate constant for the hydration process (k_{obs2}, eq 6). The direct pH jump experiments were repited for several pH values and the observed rate constants are plotted in Figure 3B. These data can be fitted to eq 6 (and eq 10 in the case of reverse pH jumps, see below) to obtain the values of k_h and k_{-h}.

Another type of information is obtained from the reverse pH jumps. In this case solutions equilibrated at moderately acidic pH values are made very acidic (see Figure 3C). The initial absorption is due to the extremely fast conversion of **A** into $\mathbf{AH}^+$. The first kinetic process is assigned to the conversion of **B** into $\mathbf{AH}^+$, because at these very acidic pH values the hydration becomes faster than tautomerization (change of regime).[25] eq 10 accounts for this step; all **B** present at pH = 5.7 react to give $\mathbf{AH}^+$ before significant changes in the **Cc** concentration take place. In other words, there is no equilibrium between **B** and **Cc** to consider and eq 10 is different from eq 6, lacking the term $1/(1 + K_t)$.[25]

$$k_{obs4} = \frac{[H^+]}{[H^+] + K_a} k_h + k_{-h}\overset{350}{\underset{351}{[H^+]}} \tag{10}$$

DOI: 10.1021/jp511537e
J. Phys. Chem. B 2015, 119, 2010−2018

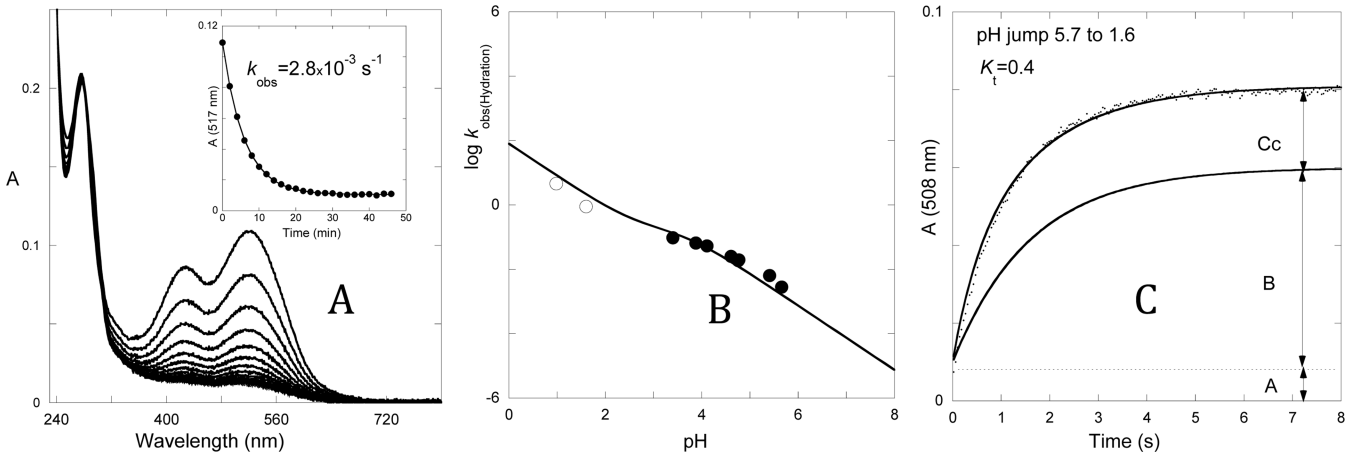

Figure 3. (A) Spectral variations upon a direct pH jump from pH= 1 to 5.7 ([Cy4′Me3glc] = 3.3×10^{-5} M). (B) pH dependence of the observed rate constant upon a direct pH jump (●); and reverse pH jump (○) of the compound cyanidin-4′-*O*-methyl-3-glucoside as a function of pH. Fitting was achieved with eq 6 for $k_h = 0.13$ s^{-1} and $k_{-h} = 85$ M^{-1} s^{-1} ($K_h = 1.5 \times 10^{-3}$ M); (C) reverse pH jump allowing to calculate $K_t = 0.4$ from the ratio of the amplitudes of the two kinetic processes, $k_{-t} = 2$ s^{-1} ([Cy4′Me3glc] = 1.6×10^{-5} M).

The second and slower step of the reverse pH jumps is assigned to the conversion of **Cc** into $\mathbf{AH}^+$ via **B** eq 11.

$$k_{obs4} = k_{-t} \tag{11}$$

The ratio of the amplitudes of the two exponentials in Figure 3C gave the values of K_t. On the other hand, fitting of eqs 6 and 10 permits to calculate k_h and k_{-h} and thus K_h. The rate constant of the slowest exponential is given by eq 11 permitting to calculate $k_{-t} = 2$ s^{-1} and from the equilibrium constant K_t the rate constant $k_t = 0.8$.

As observed in anthocyanins, the raising absorption in the near U.V. region of the spectrum indicates the formation of a small amount of **Ct** (Figure 4).

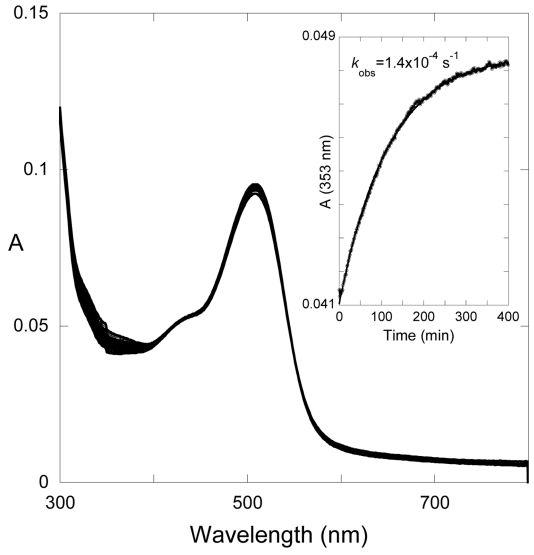

Figure 4. Spectral variations regarding the slowest processes taking place upon a direct pH jump from 1 to 3.1. ([Cy4′Me3glc] = 3.3×10^{-5} M).

The rate constant of this process, is given by eq 7. The data from Figure 2 and Figure 3 allow to calculate all the rate and equilibrium constants: from the definition of K'_a, eq 8, the equilibrium constant $K_i = 0.7$ can be obtained. Using the data resulting the fitting of eq 7 and the definition of K_i, the rate constants of the isomerization process can also be estimated, $k_i = 8.2 \times 10^{-5}$ s^{-1} and $k_{-i} = 1.2 \times 10^{-4}$ s^{-1}.

3.2.2. Cy7Gluc3glc. Figure 5A shows the absorption spectra of the compound at pH = 1.0 (flavylium cation) and after a pH jump to pH = 6.0 taken 10 ms upon addition of base. The shape and position of the spectra at pH = 6.0 is compatible with formation of the quinoidal base. The quinoidal base disappears according to a monoexponential to give the final absorption spectra showing bands in the near UV region, similarly to the data of Cy4′Me3glc, Figure 2. In the same way to the previous compound the system behaves as a single acid−base equilibrium with acidity constant $pK'_a = 1.8$ (Figure 5B).

The rate of the quinoidal disappearance is reported in Figure 6.

Fitting of the data in Figure 6 was achieved by means of eq 6 for the parameters $pK_a = 3.7$; $k_h = 0.25$ s^{-1}; $1/(1 + K_t)k_{-h} = 29$ s^{-1} M^{-1}.

The hydration process is followed by a slower one fitted with a biexponential with very small amplitude eventually due to the formation of very small amounts of *trans*-chalcone and degradation products.

A solution of Cy7Gluc3glc equilibrated at pH = 4 was used to carry out a reverse pH jump back to acid (0.3 M) with the absorption followed by stopped flow. The observed spectral variations are compatible with the transformation of basic species (A, B and *Cc*) into AH^+. (Figure 7A).

The amplitudes of the two exponentials of Figure 7B allow to calculate $K_t = 0.6$. Substituting in the data from Figure 6, $k_h = 0.25$ s^{-1} and $k_{-h} = 46$ s^{-1} M^{-1} and $K_h = 5.4 \times 10^{-3}$ M^{-1}.

Figure 7B allows evaluating the equilibrium constant K_a from the relation of the initial amplitude (all quinoidal base present is immediately transformed into flavylium cation) and the final one (total concentration transformed into flavylium cation) ca. 11% in agreement with the mole fraction predicted to **A** at the equilibrium 13% (from the ratio K_a/K'_a). As in the previous case the rate constant of the slowest process eq 11 is assigned to $k_{-t} = 3$ s^{-1}.

3.2.3. Comparison with Reference Compounds. The thermodynamic and kinetic constants determined for the two metabolites, Cy4′Me3glc and Cy7Gluc3glc, together with the data from Cy3glc, Peo3glc, Malvin, and DGF (Scheme 4) are resumed in Tables 1 and Table 2.

DOI: 10.1021/jp511537e
J. Phys. Chem. B 2015, 119, 2010−2018

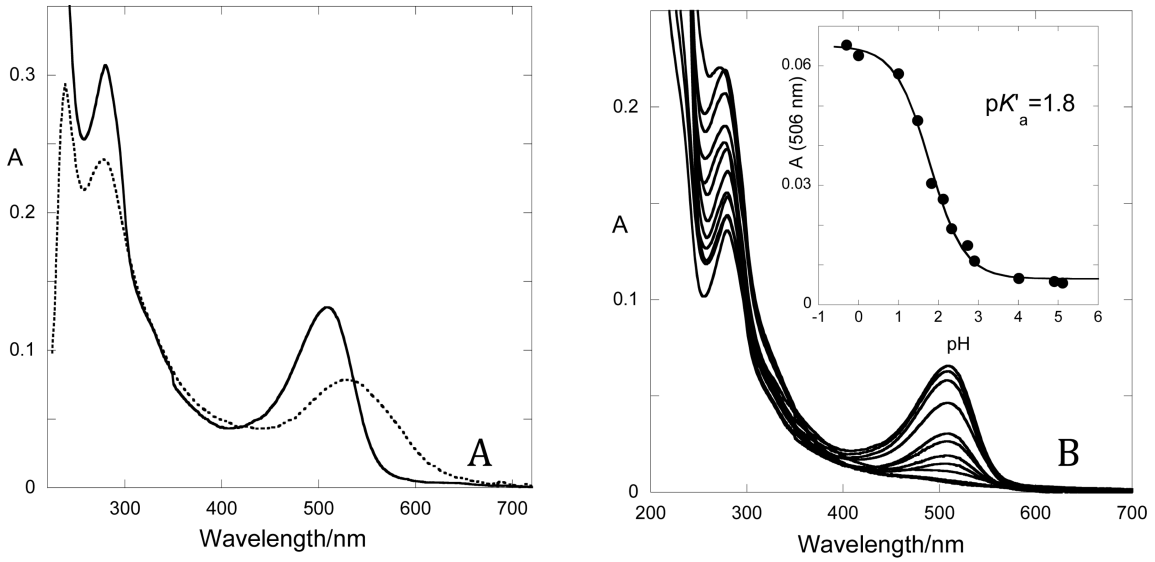

Figure 5. (A) Spectral variations of Cy7Gluc3glc (1.8×10^{-5} M) upon a pH jump from pH = 1.0 (full line) to 6.0 (traced line) obtained by stopped flow upon 10 ms of the mixing time. (B) Spectral variations of equilibrated solutions of the compound (9×10^{-6} M) as a function of pH.

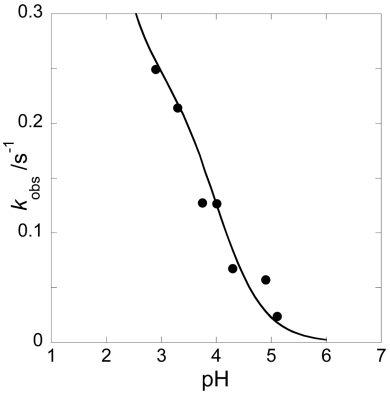

Figure 6. pH dependence of the rate constant regarding the quinoidal base disappearance upon a pH jump from equilibrated solutions at pH = 1.0 to higher pHs.

Inspection of the data from Table 1 and 2 shows that DGF behaves very differently in comparison with the other compounds. DGF bearing a glucoside in position 7 presents a much lower hydration constant and a higher isomerization constant. In effect, while in all the other compounds the main species at moderately acidic pH values is **B**, in the case of DGF, it is **Ct**.

The acidity constant to form the quinoidal base is quite similar for all the compounds suggesting that the first deprotonation takes place at the hydroxyl substituents located in ring A, by analogy with the compound 4′,7-dihydroxyflavylium where it was reported that the proton in position 7 is more acid than the one in position 4′.[28]

Cy4′Me3glc and Cy7Gluc3glc metabolites have a similar thermodynamic and kinetic behavior in comparison to Cy3glc and Peo3glc already reported,[19] except for the ring-opening-closure (which is significantly faster for the metabolites). A useful comparison is the representation of the hydration, eq 4 for

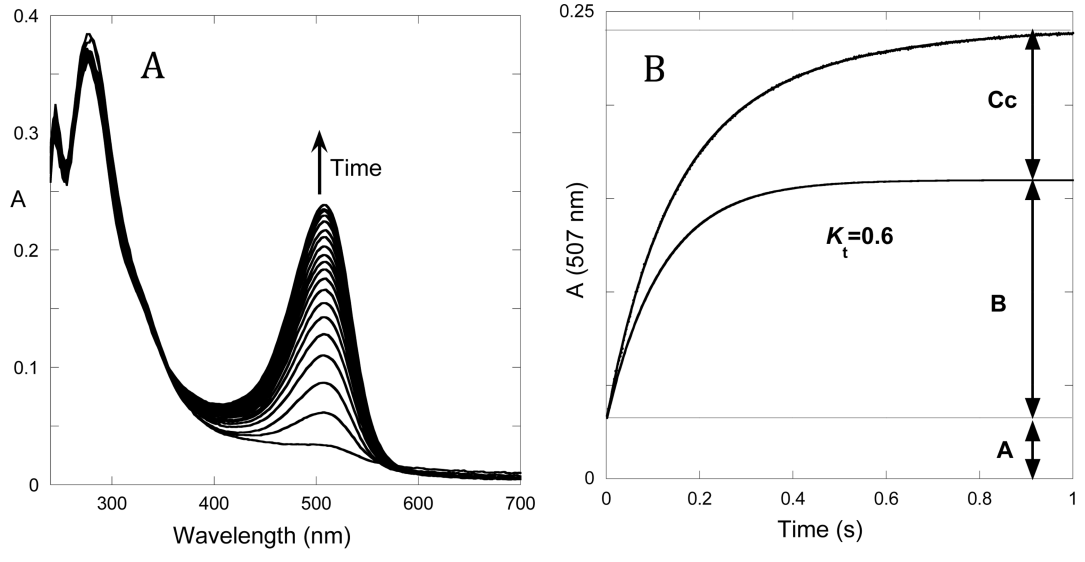

Figure 7. Spectral changes of Cy7Gluc3glc (3.7×10^{-5} M), upon a reverse pH jump from pH = 4 to $[H_3O^+]$ = 0.3 M.

DOI: 10.1021/jp511537e
J. Phys. Chem. B 2015, 119, 2010−2018

Scheme 4. Structure of Reference Compounds

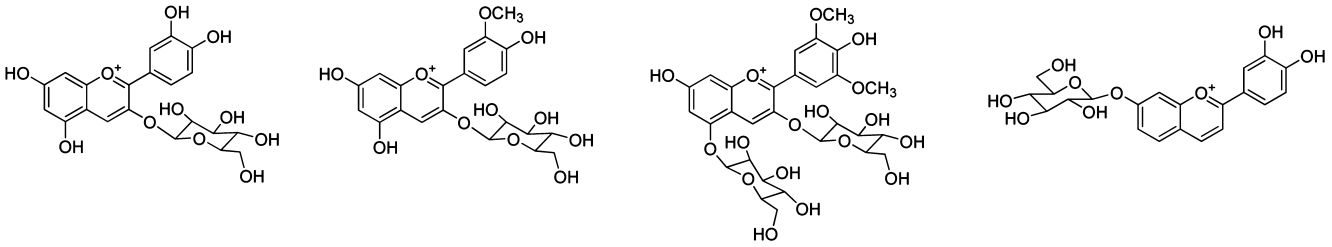

Table 1. Equilibrium Constants

	pK'_a	pK_a	K_h (M^{-1})[a]	K_t[b]	K_i[b]
Cy4′Me3glc (isopeo3glc)	2.6 ± 0.05	3.8 ± 0.1	1.5×10^{-3}	0.4	0.7
Cy7Gluc3glc	1.8 ± 0.05	3.7 ± 0.1	5.4×10^{-3}	0.6	2.16[c]
Cy3glc[19]	2.5 ± 0.05	3.8 ± 0.1	3.1×10^{-3}	0.12	–
Peo3glc[19]	2.4 ± 0.05	3.6 ± 0.1	4.9×10^{-3}	0.26	–
Malvin[26]	1.7 ± 0.05	3.2 ± 0.1	0.014	–	–
DGF[27]	2.2 ± 0.05	4.9 ± 0.1	2.5×10^{-5}	3.3	75

[a]Estimated error 10%. [b]Estimated error 20% [c]Estimated from $K_i = (K'_a - K_a - K_h - K_hK_t)/K_hK_t$.

Table 2. Rate Constants[a]

	k_h (s^{-1})[a]	k_{-h} (s^{-1})[a]	k_t (s^{-1})[b]	k_{-t} (s^{-1})[b]	k_i (s^{-1})[b]	k_{-i} (s^{-1})[b]
Cy4′Me3glc (isopeo3glc)	0.13	85	0.8	2	8.2×10^{-5}	1.2×10^{-4}
Cy7Gluc3glc	0.25	46	1.8	3	–	–
Cy3glc[19]	0.11	35	0.07	0.6	–	–
Peo3glc[19]	0.19	39	0.14	0.5	–	–
Malvin[26]	0.25	18	–	–	–	–
DGF[27]	0.33	1.4×10^4	2.6	0.8	1.2×10^{-3}	1.6×10^{-5}

[a]Estimated error 5%. [b]Estimated error 20%

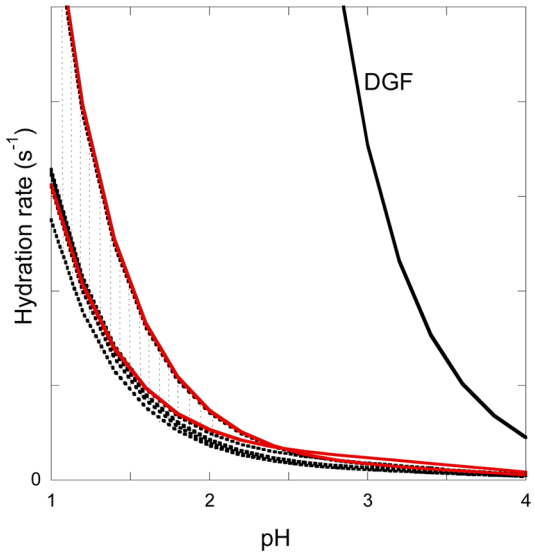

Figure 8. pH dependence of the hydration rate constant for the two metabolites reported in Table 1 and 2 (red) and DGF (black). Traced lines refer to the six most common anthocyanins-3-glucosides.[27]

anthocyanins bearing a glucoside in position 3 of the metabolites and DGF (Figure 8).

The anthocyanin monoglucosides exhibit a rate of hydration very similar except for the less substituted one callistephin (pelargonidin-3-glucoside),[27] which is close to Cy4′Me3glc. On the other hand, Cy7Gluc3glc behaves like the other anthocyanin monoglucosides. For the same pH value the rate of hydration in the case of DGF is much faster than in anthocyanins and metabolites, although in DGF the most stable species at moderately acidic pH values is **Ct** and not **B**. In other words, a faster hydration to give **B**, does not mean a greater stability for this species.

4. CONCLUSION

This work allowed us to characterize the equilibrium network of two anthocyanin metabolites with in vivo occurrence. This knowledge is very useful to understand which species forms of these metabolites are present at different in vivo pH environments in pharmacokinetic studies.

AUTHOR INFORMATION

Corresponding Authors

*(V.d.F.) E-mail: vfreitas@fc.up.pt.
*(F.P.) E-mail: fp@fct.unl.pt.

Notes

The authors declare no competing financial interest.

ACKNOWLEDGMENTS

L.C. and N.B. gratefully acknowledge the postdoc grants from Fundação para a Ciência e Tecnologia (FCT), Nos. SFRH/BPD/72652/2010 and SFRH/BPD/84805/2012, respectively. The authors would like to thank the NMR Lab at CEMUP supported by the Project NORTE-07-0162-FEDER-000048.

DOI: 10.1021/jp511537e
J. Phys. Chem. B 2015, 119, 2010−2018

REFERENCES

(1) Cheynier, V. Polyphenols in Foods Are More Complex Than Often Thought. *Am. J. Clin. Nutr.* **2005**, *81*, 223−229.

(2) Hou, D. X. Potential Mechanisms of Cancer Chemoprevention by Anthocyanins. *Curr. Mol. Med.* **2003**, *3*, 149−159.

(3) Katsube, N.; Iwashita, K.; Tsushida, T.; Yamaki, K.; Kobori, M. Induction of Apoptosis in Cancer Cells by Bilberry (Vaccinium Myrtillus) and the Anthocyanins. *J. Agric. Food. Chem.* **2003**, *51*, 68−75.

(4) Pool-Zobel, B. L.; Bub, A.; Schröder, N.; Rechkemmer, G. Anthocyanins Are Potent Antioxidants in Model Systems but Do Not Reduce Endogenous Oxidative DNA Damage in Human Colon Cells. *Eur. J. Nutr.* **1999**, *38*, 227−234.

(5) Satué-Gracia, M. T.; Heinonen, M.; Frankel, E. N. Anthocyanins as Antioxidants on Human Low-Density Lipoprotein and Lecithin-Liposome Systems. *J. Agric. Food. Chem.* **1997**, *45*, 3362−3367.

(6) Wang, H.; Cao, G.; Prior, R. L. Oxygen Radical Absorbing Capacity of Anthocyanins. *J. Agric. Food. Chem.* **1997**, *45*, 304−309.

(7) Neuhouser, M. L. Dietary Flavonoids and Cancer Risk: Evidence from Human Population Studies. *Nutr. Cancer* **2004**, *50*, 1−7.

(8) Passamonti, S.; Vrhovsek, U.; Vanzo, A.; Mattivi, F. The Stomach as a Site for Anthocyanins Absorption from Food. *FEBS Lett.* **2003**, *544*, 210−213.

(9) Talavéra, S.; Felgines, C.; Texier, O.; Besson, C.; Manach, C.; Lamaison, J. L.; Rémésy, C. Anthocyanins Are Efficiently Absorbed from the Small Intestine in Rats. *J. Nutr.* **2004**, *134*, 2275−2279.

(10) Felgines, C.; Talavera, S.; Gonthier, M. P.; Texier, O.; Scalbert, A.; Lamaison, J. L.; Remesy, C. Strawberry Anthocyanins Are Recovered in Urine as Glucuro- and Sulfoconjugates in Humans. *J. Nutr.* **2003**, *133*, 1296−301.

(11) Kay, C. D.; Mazza, G.; Holub, B. J.; Wang, J. Anthocyanin Metabolites in Human Urine and Serum. *Br. J. Nutr.* **2004**, *91*, 933−42.

(12) Wu, X.; Cao, G.; Prior, R. L. Absorption and Metabolism of Anthocyanins in Elderly Women after Consumption of Elderberry or Blueberry. *J. Nutr.* **2002**, *132*, 1865−71.

(13) Brouillard, R.; Delaporte, B. Chemistry of Anthocyanin Pigments 0.2. Kinetic and Thermodynamic Study of Proton-Transfer, Hydration, and Tautomeric Reactions of Malvidin 3-Glucoside. *J. Am. Chem. Soc.* **1977**, *99*, 8461−8468.

(14) Pina, F.; Melo, M. J.; Laia, C. A. T.; Parola, A. J.; Lima, J. C. Chemistry and Applications of Flavylium Compounds: A Handful of Colours. *Chem. Soc. Rev.* **2012**, *41*, 869−908.

(15) Melo, M. J.; Sousa, M.; Parola, A. J.; de Melo, J. S. S.; Catarino, F.; Marcalo, J.; Pina, F. Identification of 7,4 ′-Dihydroxy-5-Methoxy-flavylium in "Dragon's Blood": To Be or Not to Be an Anthocyanin. *Chem.—Eur. J.* **2007**, *13*, 1417−1422.

(16) Cruz, L.; Mateus, N.; de Freitas, V. First Chemical Synthesis Report of an Anthocyanin Metabolite with in Vivo Occurrence: Cyanidin-4′-O-Methyl-3-Glucoside. *Tetrahedron Lett.* **2013**, *54*, 2865−2869.

(17) Bakstad, E. *Method for the Synthesis of Anthocyanins*; BIOSYNTH AS: Sandnes, Norway, 2009.

(18) Küster, W. F.; Thiel, A. *Tabelle per le Analisi Chimiche e Chimico-Fisiche*; 12th ed.; Hoepli: Milan, Italy, 1982.

(19) Leydet, Y.; Gavara, R.; Petrov, V.; Diniz, A. M.; Jorge Parola, A.; Lima, J. C.; Pina, F. The Effect of Self-Aggregation on the Determination of the Kinetic and Thermodynamic Constants of the Network of Chemical Reactions in 3-Glucoside Anthocyanins. *Phytochemistry* **2012**, *83*, 125−135.

(20) Mora-Soumille, N.; Al Bittar, S.; Rosa, M.; Dangles, O. Analogs of Anthocyanins with a 3′,4′-Dihydroxy Substitution: Synthesis and Investigation of Their Acid−Base, Hydration, Metal Binding and Hydrogen-Donating Properties in Aqueous Solution. *Dyes Pigments* **2013**, *96*, 7−15.

(21) Fernandes, I.; Azevedo, J.; Faria, A.; Calhau, C.; de Freitas, V.; Mateus, N. Enzymatic Hemisynthesis of Metabolites and Conjugates of Anthocyanins. *J. Agric. Food. Chem.* **2009**, *57*, 735−745.

(22) Brouillard, R.; Dubois, J. E. Mechanism of Structural Transformations of Anthocyanins in Acidic Media. *J. Am. Chem. Soc.* **1977**, *99*, 1359−1364.

(23) Brouillard, R.; Lang, J. The Hemiacetal-Cis-Chalcone Equilibrium of Malvin, a Natural Anthocyanin. *Can. J. Chem.* **1990**, *68*, 755−761.

(24) Pina, F. Chemical Applications of Anthocyanins and Related Compounds. A Source of Bioinspiration. *J. Agric. Food. Chem.* **2014**, *62*, 6885−6897.

(25) Pina, F. Anthocyanins and Related Compounds. Detecting the Change of Regime between Rate Control by Hydration or by Tautomerization. *Dyes Pigments* **2014**, *102*, 308−314.

(26) Pina, F. Thermodynamics and Kinetics of Flavylium Salts - Malvin Revisited. *J. Chem. Soc., Faraday Trans.* **1998**, *94*, 2109−2116.

(27) Petrov, V.; Gavara, R.; Dangles, O.; Al Bittar, S.; Mora-Soumille, N.; Pina, F. A Flash Photolysis and Stopped-Flow Spectroscopy Study of 3 ′,4 ′-Dihydroxy-7-O-Beta-D-Glucopyranosyloxyflavylium Chloride, an Anthocyanin Analogue Exhibiting Efficient Photochromic Properties. *Photochem. Photobiol. Sci.* **2013**, *12*, 576−581.

(28) Jurd, L.; Geissman, T. A. Anthocyanins and Related Compounds. Ii. Structural Transformations of Some Anhydro Bases. *J. Org. Chem.* **1963**, *28*, 2394−2397.

DOI: 10.1021/jp511537e
J. Phys. Chem. B 2015, 119, 2010−2018